AIP | Review of Scientific Instruments

Vacuum insulation of the high energy negative ion source for fusion applicationa)

A. Kojima, M. Hanada, A. Hilmi, T. Inoue, K. Watanabe, M. Taniguchi, M. Kashiwagi, N. Umeda, H. Tobari, S. Kobayashi, Y. Yamano, and L. R. Grisham

Citation: Review of Scientific Instruments **83**, 02B117 (2012); doi: 10.1063/1.3672471
View online: http://dx.doi.org/10.1063/1.3672471
View Table of Contents: http://scitation.aip.org/content/aip/journal/rsi/83/2?ver=pdfcov
Published by the AIP Publishing

Vacuum insulation of the high energy negative ion source for fusion application[a)]

A. Kojima,[1,b)] M. Hanada,[1] A. Hilmi,[2] T. Inoue,[1] K. Watanabe,[1] M. Taniguchi,[1] M. Kashiwagi,[1] N. Umeda,[1] H. Tobari,[1] S. Kobayashi,[2] Y. Yamano,[2] and L. R. Grisham[3]

[1]*Japan Atomic Energy Agency, Naka, Ibaraki 311-0193, Japan*
[2]*Saitama University, Saitama, Saitama-ken, 338-8570, Japan*
[3]*Princeton Plasma Physics Laboratory, Princeton, New Jersey 08543, USA*

(Presented 13 September 2011; received 9 September 2011; accepted 15 November 2011; published online 16 February 2012)

Vacuum insulation on a large size negative ion accelerator with multiple extraction apertures and acceleration grids for fusion application was experimentally examined and designed. In the experiment, vacuum insulation characteristics were investigated in the JT-60 negative ion source with >1000 apertures on the grid with the surface area of ~2 m^2. The sustainable voltages varied with a square root of the gap lengths between the grids, and decreased with number of the apertures and with the surface area of the grids. Based on the obtained results, the JT-60SA (super advanced) negative ion source is designed to produce 22 A, 500 keV D^- ion beams for 100 s. © *2012 American Institute of Physics*. [http://dx.doi.org/10.1063/1.3672471]

I. INTRODUCTION

In order to heat fusion plasmas and drive plasma current efficiently, high energy negative ion sources are utilized in advanced neutral beam injectors for nuclear fusion devices, such as JT-60 super advanced (SA),[1] ITER,[2] and large helical device[3] whose beam energies are 500 keV, 1 MeV, and 190 keV, respectively. These negative ion sources for fusion are characterized by large size grids with multiple apertures for ion extraction and multiple stages for high energy beam production. In order to achieve high-power and long-pulse negative ion beams, lots of effort has been expended so far.[4]

One of the high energy negative ion sources having negative ion current over 10 A is the JT-60 negative ion source, which has been constructed as the first practical negative ion source for neutral beam injection into fusion plasma, and has been designed to produce 500 keV, 22 A negative ion beams for 10 s by using a 3-stage accelerator.[5] The key issues of the JT-60U ion source to produce high-power and long-pulse beams were grid heat load and voltage holding capability.[6,7] As a result of tuning the gap lengths between the acceleration grids[8] and optimizing beam radiation shield[9] to increase the voltage holding of the accelerator, 500 keV, ~3 A beams have been produced.[8] Based on these results, the JT-60SA ion source is being designed by modifying the JT-60U ion source.[10]

As for the vacuum insulation design, the key parameter of the JT-60 ion source has not been clarified in the previous results. In terms of the electric field profile, >1000 apertures on the 2 m^2 large grids in the JT-60 ion source cause the locally strong and largely flat electric field profiles, in which highest electric field is 3–4 times larger than that of flat regions. In addition, the ITER ion source, specified for 1 MeV, 40 A beams, has similar size and configuration of the multi-stage accelerator to the JT-60 ion source.[11] For the designs of such large grids with multi-apertures for fusion application, a database of vacuum insulation with locally strong electric field profile is required because previous databases are not adequate to estimate the voltage holding capability.[8,9,12–14]

Therefore, the influence of the multi-apertures and large grid area on the voltage holding capability has been examined with the JT-60U ion source (~2 m^2) and with small electrodes (~0.02 m^2) having multi-apertures. In this paper, the obtained characteristics of the vacuum insulation of the large grids with multi-apertures are described. In addition, the vacuum insulation design for the JT-60SA ion source based on the obtained database is reported.

II. EXPERIMENTAL SETUP

The JT-60U ion source is composed of an arc chamber and the 3-stage accelerator as shown in Fig. 1(a). In this experiment, negatively charged high voltage is applied to each stage of the ion source with a typical pressure of 1×10^{-4} Pa by a power supply with a capability of 300 kV and 10 mA. Each acceleration stage is insulated by a large fiber-reinforced plastic ring with a diameter of 1.8 m. In the ion source, the acceleration grids (0.45 m × 1.1 m), made of oxygen free copper, are mounted on 1500 mm grid supports made of stainless steel and aluminum alloy. These grid supports are installed coaxially. In the case of the rated acceleration voltage of 500 kV, a strong electric field of 5–9 kV/mm is observed at 1100 (1080 + 20 adjusting aperture) apertures of the acceleration grids and at the corners of the grid supports.

In order to design the vacuum insulation of the JT-60SA ion source, the effect of the electric field profile has been

[a)]Contributed paper, published as part of the Proceedings of the 14th International Conference on Ion Sources, Giardini Naxos, Italy, September 2011.
[b)]Author to whom correspondence should be addressed. Electronic mail: kojima.atsushi@jaea.go.jp.

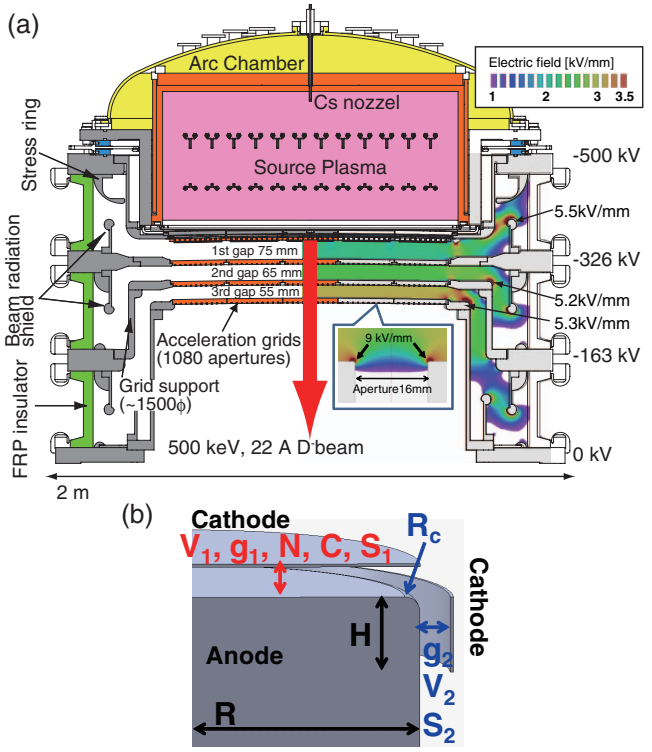

FIG. 1. (Color online) The JT-60U negative ion source with the 3-stage accelerator. Electric field profile calculated by ESTAT (a) Field precision is also shown in the right side. An enlarged view shows the electric field profile on a grid aperture. (b) Simple model of the design parameter for the acceleration grid and coaxial grid support structure.

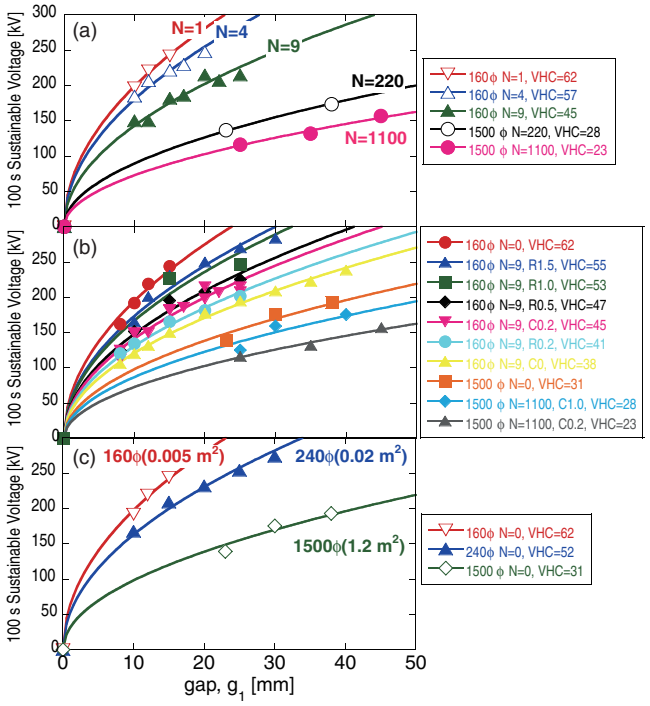

FIG. 2. (Color online) Relation between sustainable voltages and gap lengths (a) by changing aperture number N, (b) by changing shape of aperture edge. (C: chamfer-taper, R: rounded-taper), and (c) by changing grid surface area without aperture.

investigated. This electric field profile is determined by the following parameters of the acceleration grid which is simply modeled as shown in Fig. 1(b). Basically, the sustainable voltage of the single-stage is determined by the lowest value of voltage holding at the acceleration gap (V_1) and the grid support (V_2). As for V_1, it is determined by the gap length g_1, the aperture number N, the shape of aperture edge C, and the surface area S_1 corresponding to the grid diameter R. As for V_2, it is determined by the gap length g_2, the curvature of the grid support R_c, and the surface area S_2 corresponding to R and the overlap length H for the coaxial configuration. Introducing these characteristic design parameters, the dependences of sustainable voltages on these parameters have been investigated by changing g_1 and gap lengths of the JT-60U ion source and the small electrodes, respectively.

In this experiment, the aperture number of the acceleration grids was varied by covering the apertures with plates of 1 mm thickness made of stainless steel. In order to obtain the database with lower aperture number and smaller grid-size than that of the JT-60 ion source, the small electrodes with diameters of 160 mm[14] and 240 mm were also utilized. In these electrodes, the 160 mm electrodes have 1–9 apertures whose diameter is the same size as that of the JT-60 negative ion source. Moreover, these electrodes have various electric field profiles around the apertures, which are caused by change of the shape of the aperture edge.

III. EXPERIMENTAL RESULTS

Figure 2 shows the experimental results of various grids and small electrodes. The sustainable voltage is defined to be the voltage whose breakdown probability is 0% in repeat of 10–20 high voltage pulses for 100 s in vacuum. As previously reported, the experimental results indicated that the sustainable voltages increased as a function of ${g_1}^{0.5}$ which was similar to the Clump law (EV = const.)[15] where E is the electric field and V is the applied voltage. In order to investigate the dependence on the design parameters, the voltage holding capability (VHC) is defined to be the coefficient of g_1 dependence as $V(g_1)/{g_1}^{0.5}$ in units of kV/mm$^{0.5}$.

At first, VHC for V_1 was investigated by changing aperture number N, the shape of aperture edge C and the grid surface area S with $g_1 < 50$ mm, because the sustainable voltage of the ion source had been saturated by V_2 in the case of $g_1 > 50$ mm.[8] After that, V_2 was investigated by changing g_2.

A. Dependence on aperture number N (Area effect with strong electric field)

Figure 2(a) shows the relation between V_1 and g_1 by changing N up to 1100 by using the multi-apertures grids. The shape of the aperture edge C is chamfer-taper of 0.2 mm (C = C0.2 mm). The VHC was decreased with N as a function of VHC = $67N^{-0.15}$ as shown in Fig. 3. This reduction of the VHC is because the area of the higher electric field generated around the aperture edge increases with number of the apertures. V_1 is found to be determined by this effect. However, the experimental results also showed that VHCs in N

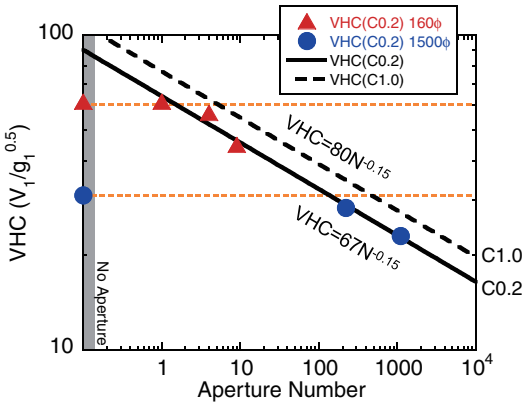

FIG. 3. (Color online) Effect of the area with strong electric field generated around multi-apertures on VHC.

< 100 for 1500 mm grid and $N < 1$ for 160 mm electrodes tended to become constant. This tendency can be considered as follows. When the total area giving higher electric field around apertures becomes relatively small with respect to the flat area without apertures, the VHC is dominated by the influence from the flat region, which is so-called area effect.[12]

As a result, it was found that VHC of the ion source with $N = 1100$ was strongly dominated by the locally strong electric field profile caused by apertures. The obtained N dependence is applied to the estimation of V_1 and the design of the JT-60SA ion source later.

B. Dependence on shape of aperture edge C (Profile effect of local electric field)

Figure 2(b) shows the relation between V_1 and g_1 by changing C of the chamfer- or rounded-tapers around the aperture edges. This dependence can be considered to be determined not by the peak electric field but by the local electric field profile (area integral of electric field), because the VHC at $N = 9$, $C =$ C0.2 mm (Chamfer-taper) is higher than that at $N = 9$, $C =$ R0.2 mm (Rounded-taper) even though the peak electric field strength of C0.2 mm is higher than that of R0.2 mm as shown in Fig. 4(a). By taking the effect of the electric field profile into account, the VHC is shown as a function of ES as shown in Fig. 4(b), where ES is the area integral of the electric field up to $R = 9.5$ mm which is determined by the aperture arrangement as shown in Fig. 4(a). In order to compare 1500 mm grids with 160 mm electrodes, both the VHC and ES are normalized by that at the values of $C =$ C0.2 mm. As a result, the VHC is linearly decreased with the ES except for $C =$ R1.5 mm. The impact of the aperture edge with $C =$ R1.5 mm is not clear because the profile E_{max}/E_{flat} is wide and the maximum value is less than 1.5, which is lower than that of $C =$ R1.0 mm having $E_{max}/E_{flat} \sim 2$.

The JT-60U ion source has $N = 1100$, $C =$ C0.2 mm apertures in 1st and 2nd gaps. $N = 1100$, $C =$ C1.0 mm apertures are only equipped with 3rd gap. From the obtained N and C dependences, VHC of V_1 on 3rd gap is estimated to be $80N^{-0.15}$ which is 20% higher than that of 2nd gap as shown in Fig. 3.

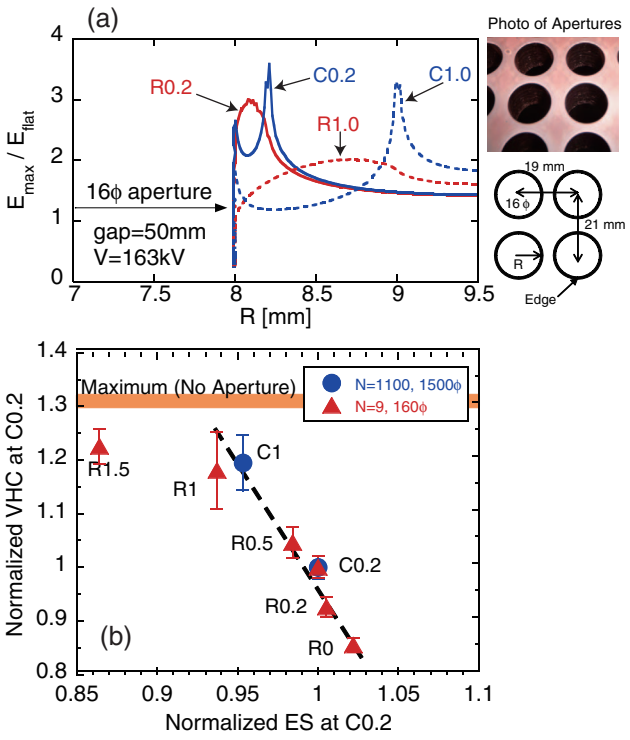

FIG. 4. (Color online) (a) Electric field profiles on chamfer- and rounded-tapers of 0.2 mm and 1.0 mm, respectively. Aperture arrangement is shown together. (b) Effect of electric field profile on VHC.

C. Dependence on surface area *S* (Area effect with flat electric field)

Figure 2(c) shows the relation between V_1 and g_1 by changing S_1, where the 1500 mm grid (1.2 m^2) and 160 mm (0.005 m^2) and 240 mm (0.02 m^2) electrodes have been utilized without apertures ($N = 0$). These S_1 were estimated from the grid diameters R according to Fig. 1(b). This S_1 dependence is considered to be the area effect with the weak electric field on a flat region as mentioned above. The results obtained indicated that VHC $= 32{S_1}^{-0.125}$ as shown in Fig. 5(a), which was weaker than the previously reported area effect.[12]

By applying the S dependence to the large acceleration grids with the coaxial structure as shown in Fig. 1(b), the relation between g_2/g_1, H/R and V_2/V_1 was calculated in terms of the area effect (S dependence), where g_2/g_1 and H/R indicate the gap ratio and size ratio, respectively. As a result, $g_2 = R\{\exp(g_1/AR)-1\}$ is required for $V_2/V_1 = 1$, where $A = (2H/R)^{-0.25}$. Figure 5 shows the calculated contour map of V_2/V_1 as a function of g_2/g_1 and H/R; here, g_2/g_1 and H/R of the JT-60U ion source is shown together. For example, the original JT-60U ion source had $V_2/V_1 \sim 1.2$ at $g_2/g_1 \sim 1.2$. However, when g_1 of the 3rd gap in the JT-60U ion source was increased from the original values (red circle), V_2/V_1 was decreased to less than 1 with decreasing g_2/g_1, which suggested that the sustainable voltage was saturated by V_2 at the grid support. This phenomenon has been observed in the previous results.[8] However, the effect from the local electric field at R_c was not understood in the previous experiment.

In order to design the acceleration grids, g_2/g_1 and H/R should be optimized to give the condition of $V_2/V_1 > 1$.

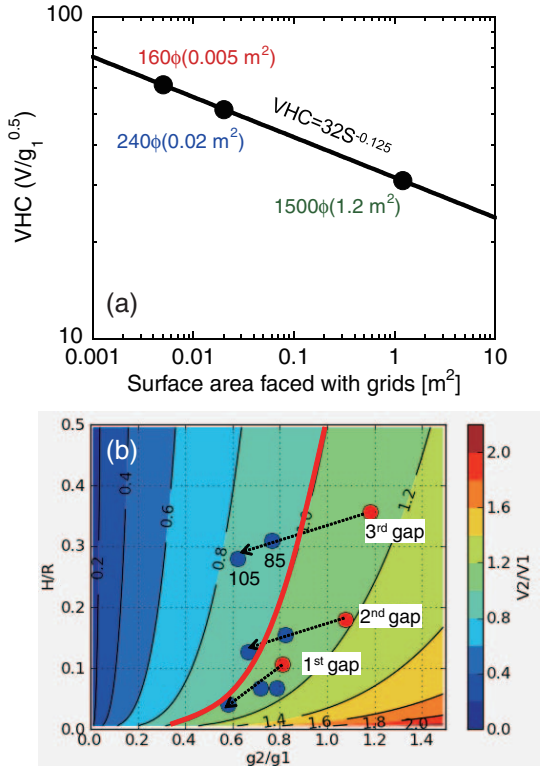

FIG. 5. (Color online) (a) Effect of area with weak electric field generated on flat surface on VHC. (b) Calculation results for the relation between V_2/V_1 and g_2/g_1. The trajectories in gap scan experiments with the JT-60U ion source are shown together.

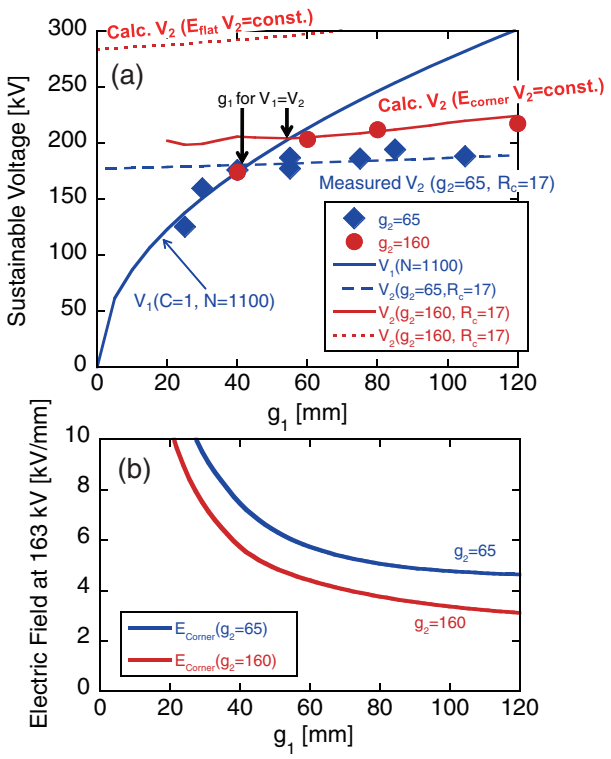

FIG. 6. (Color online) (a) Sustainable voltage restricted by the grid support with $g_2 = 65$ and 160 mm, respectively. Calculations of V_2 from the condition of EV = const and area effect are shown together. (b) Highest electric field strengths at corner of the grid support and at aperture edge.

However, since a certain value of H/R is necessary for the coaxial structure which comes from the different VHC for the vacuum gaps and the FRP insulators, g_2/g_1 should be selected to be 1.2 which was enough to maintain the condition of $V_2/V_1 > 1$. In this result, it is noted that the effect of the local electric field at R_c is not included. In addition, V_1 determined by N dependence becomes lower than that of S dependence, which results in an extra margin of 25%.

D. Restriction by grid support V_2

V_2 has been examined to obtain the design basis for R_c and g_2 experimentally. As reported in the previous paper,[8] the sustainable voltage is limited by V_2 in $g_1 > 50$ mm as shown in Fig. 6(a), and the measured V_2 was about 180 kV in the original configuration. In order to investigate the effect of the local electric field at R_c on V_2, g_2 of the JT-60U ion source has been increased from the original value of 65 mm to 160 mm.

When g_2 is extended, measured V_2 is considered to be increased with g_2 according to EV_2 = constant, where there are two electric fields generated on the grid support. One is the electric field in the flat region (E_{flat}) which depends on g_2. The calculated V_2 from the relation of $E_{flat}V_2$ = constant is shown as a higher value in Fig. 6(a). The other is the electric field at the corner of the grid support (E_{corner}) which is determined by R_c and g_2 and is saturated in $g_1 > 50$ mm as shown in Fig. 6(b). The calculated V_2 from the relation of $E_{corner}V_2$ = constant is shown as a lower value in Fig. 6(a).

As a result, the experimental results showed good agreement with the calculation from the lower V_2, which comes from $E_{corner}V_2$ = const. Therefore, V_2 was found to be saturated by the local electric field at the corner of the grid support. In the case of the JT-60U ion source, $R_c = 17$ mm is selected as the original value. In order to achieve $V_2/V_1 > 1$ in $g_1 > 50$ mm, the increases of R_c and g_2 are required according to experimental results. In addition, because both of the sustainable voltages with $g_2 = 65$ mm, 170 mm were similar at $g_1 = 40$ mm, it was found that the local electric field at R_c did not have an affect on V_1.

IV. VACUUM INSULATION DESIGN

The vacuum insulation of the JT-60SA ion source is designed by applying the obtained database for large grids with the multiple-apertures.

At first, the dependence of g_1, N, and C dependences are taken into account so as to achieve a sustainable voltage V_1 of 200 kV across each acceleration stage. Therefore, the total acceleration voltage defined by 3 V_1 = 600 kV gives a 20% margin to the rated voltage of 500 kV. This margin is required from the uncertainty of the multi-stage effect in multi-stage accelerators. Moreover, reduction of the sustainable voltage due to beam acceleration has been experienced, which is about 15 kV at minimum.[8] Fig. 7(a) shows the previous results of the JT-60U ion source with the 500 kV power

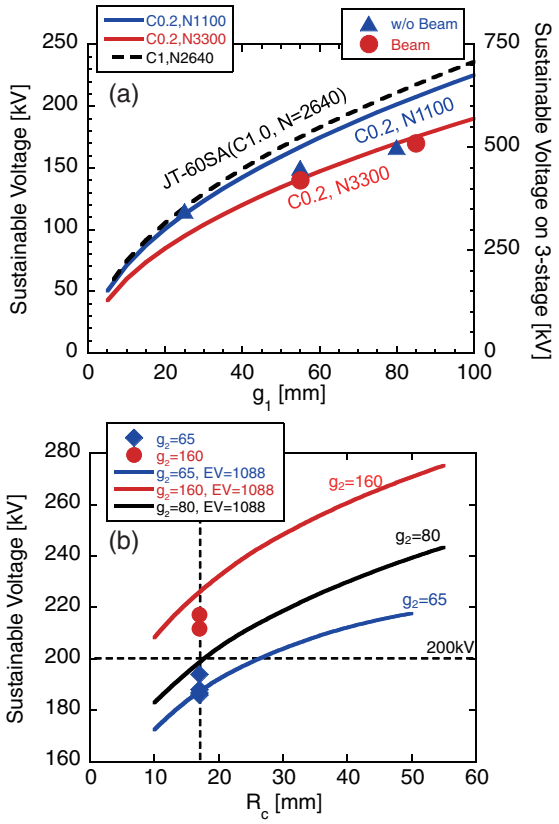

FIG. 7. (Color online) Experimental results and calculations of (a) voltage holding tests with the 3-stage accelerator and (b) the relation between sustainable voltage and R_c at the corner of the grid support.

supply, where g_1 denotes the minimum g_1 in the 3-stage acceleration gaps. g_1 of 55 mm and 85 mm are the gap lengths of the original and modified ion sources, respectively. A value of g_1 of 25 mm has been also investigated in the test stand. In the case of 3-stages, the ratio of the area with strong electric field and the flat area is the same as for a single-stage. Therefore, the impact of the locally strong electric field profile caused by the apertures is larger than that of surface area. Because the acceleration voltage is applied to 3-stages serially, the total N in the ion source can be considered to be 3300, which may cause the multi-stage effect.

In the JT-60SA ion source, N is designed to be reduced to 80% of the JT-60U ion source, because the non-uniformity of the source plasma has limited the useful beam extraction region. In addition, $C = $ C1.0 mm is applied to improve VHC. Therefore, VHC of the JT-60SA ion source is estimated to be 28 for an individual acceleration stage ($N = 880$), and at least 24 for the full 3-stage accelerator ($N = 2640$). After all, g_1 of 70 mm is enough to satisfy the condition of $V_1 \sim 200$ kV and the rated acceleration voltage, which includes the margin to account for the multi-stage effect.

Next, g_2 and R_c are designed to satisfy the condition of $V_2/V_1 > 1$ at $V_1 \sim 200$ kV. Figure 7(b) shows the relation between V_2, R_c, and g_2. This relation was extrapolated by the condition of $EV_2 = $ const, where E denotes the local electric field at R_c. In addition, $g_2/g_1 \sim 1.2$ is required from the analysis about the area effect. Therefore, $R_c = 30$ mm with $g_2 = 65$ mm or $R_c = 17$ mm with $g_2 = 80$ mm are enough to satisfy the condition of $V_2 > 200$ kV. Rough approximation suggested that $R_c + g_2 \sim 100$ mm was necessary to obtain $V_2 \sim 200$ kV.

As a result, the vacuum insulation for JT-60SA ion source has been designed by the experimentally obtained database for the large girds with multi-apertures. The detail designs including the beam steering and the engineering analysis are future works.

ACKNOWLEDGMENTS

The authors are much indebted to the JT-60 NBI group for their continuous support.

[1]M. Hanada, N. Akino, Y. Endo, and T. Inoue, *et al.*, J. Plasma Fusion Res. **9**, 208 (2010).
[2]R. Hemsworth, H. Decamps, and J. Graceffa, *et al.*, Nucl. Fusion **49**, 045006 (2009).
[3]Y. Takeiri, S. Morita, and K. Ikeda, *et al.*, Nucl. Fusion **47**, 1078 (2007).
[4]Y. Takeiri, Rev. Sci. Instrum. **81**, 02B114 (2010)
[5]M. Kuriyama, N. Akino, and N. Ebisawa, *et al.*, Fusion Sci. Technol. **42**, 410 (2002).
[6]A. Kojima, M. Hanada, Y. Tanaka, and T. Inoue, *et al.*, Rev. Sci. Instrum. **81**, 02B112 (2010).
[7]M. Hanada, Y. Ikeda, L. Grisham *et al.*, *IAEA Fusion Energy Conference* 2008, FT/P2-27.
[8]A. Kojima, M. Hanada, Y. Tanaka, M. Kawai, N. Akino, M. Kazawa, M. Komata, K. Mogaki, K. Usui, S. Sasaki, K. Kikuchi, N. Seki, S. Nemoto, K. Oshima, T. Simizu, N. Kubo, K. Oasa, T. Inoue, K. Watanabe, M. Taniguchi, M. Kashiwagi, H. Tobari, N. Umeda, S. Kobayashi, Y. Yamano, and L. R. Grisham, Nucl. Fusion **51**, 083049 (2011).
[9]A. Kojima, M. Hanada, Y. Tanaka, M. Taniguchi, M. Kashiwagi, T. Inoue, N. Umeda, K. Watanabe, H. Tobari, S. Kobayashi, Y. Yamano, L. R. Grisham, and JT-60 NBI group, AIP Conf. Proc. **1390**, 466 (2011).
[10]M. Hanada, A. Kojima, T. Inoue, K. Watanabe, M. Taniguchi, M. Kashiwagi, H. Tobari, N. Umeda, N. Akino, M. Kazawa, K. Oasa, M. Komata, K. Usui, K. Mogaki, S. Sasaki, K. Kikuchi, S. Nemoto, K. Ohshima, Y. Endo, T. Simizu, N. Kubo, M. Kawai, and L. R. Grisham, AIP Conf. Proc. **1390**, 536 (2011).
[11]M. Kashiwagi, M. Taniguchi, M. Dairaku, H. P. L. de Esch, L. R. Grisham, L. Svensson, H. Tobari, N. Umeda, K. Watanabe, K. Sakamoto, and T. Inoue, Nucl. Fusion **49**, 065008 (2009).
[12]J. M. Lafferty, *Vauum Arcs, Theory and Application* (Wiley, New York, 1980).
[13]F. Bottiglioni and J. P. Bussac, Physica **104C**, 248 (1981).
[14]K. Watanabe, M. Mizuno, Y. Ohara, M. Tanaka, K. Kobayashi, E. Takahashi, and T. Uede, J. Appl. Phys. **72**, 3949 (1992).
[15]L. Cranberg, J. Appl. Phys. **23**, 518 (1952).